Fine Structure of Nearly Isotropic Bright Excitons in InP/ZnSe Colloidal Quantum Dots Supporting Information

Annalisa Brodu,[†,⊥] Vigneshwaran Chandrasekaran,[‡,¶,⊥] Lorenzo Scarpelli,[§] Jonathan Buhot,[‖] Francesco Masia,[§] Mariana V. Ballottin,[‖] Marion Severijnen,[‖] Mickaël D. Tessier,[‡,¶] Dorian Dupont,[‡,¶] Freddy T. Rabouw,[†] Peter C.M. Christianen,[‖] Celso de Mello Donega,[†] Daniël Vanmaekelbergh,[*,†] Wolfgang Langbein,[*,§] and Zeger Hens[*,‡,¶]

Debye Institute for Nanomaterials Science, Utrecht University, The Netherlands, Physics and Chemistry of Nanostructures, Ghent University, Ghent, Belgium, Center for Nano and Biophotonics, Ghent University, Belgium, School of Physics and Astronomy, Cardiff University, Cardiff, United Kingdom, and High Field Magnet Laboratory, HFML-EMFL, Radboud University, The Netherlands

E-mail: d.vanmaekelbergh@uu.nl; langbeinww@cardiff.ac.uk; zeger.hens@ugent.be

[*]To whom correspondence should be addressed
[†]Debye Institute for Nanomaterials Science, Utrecht University
[‡]Physics and Chemistry of Nanostructures, Ghent University
[¶]Center for Nano and Biophotonics, Ghent University
[§]School of Physics and Astronomy, Cardiff University, Cardiff, United Kingdom
[‖]High Field Magnet Laboratory, Radboud University
[⊥]Contributed equally to this work

Contents

S1 Synthesis protocol

The InP/ZnSe QDs studied in this work were synthesised using the general methods described by Tessier *et al.*[1] To obtain 10-nm core/shell structures with a 3.2-nm cores, the following procedure was applied. 50 mg (0.23 mmol) of indium(III) chloride and 150 mg (1.1 mmol) of zinc(II) chloride are first mixed in 2.5 mL (7.5 mmol) of technical oleylamine (OLA). The reaction mixture is stirred and degassed at 120 °C for an hour and then heated to 180 °C under inert atmosphere. Upon reaching 180 °C, the synthesis of InP nanocrystals is initiated by quickly injecting a volume of 0.23 mL (0.8 mmol) of tris(diethylamino)phosphine in the above mixture. After a reaction time of 20 min, 3.2-nm InP QD cores are formed. The formation of the ZnSe shell is initiated by injecting 0.45 ml of stoichiometric TOP-Se (2.24 M). At 140 min, a mixture of 2 g (3 mmol) of $Zn(stearate)_2$, 8 mL of octadecene (ODE) and 2 mL of OLA is injected. The temperature is increased from 180 °C to 320 °C and 1.4 ml of TOP-Se is injected drop by drop during the rise of temperature. At 240 min, the reaction is stopped. InP/ZnSe QDs are then precipitated once in ethanol and suspended in toluene.

S2 Micro-Photoluminescence Analysis

For single dot μ-PL, the quartz cover slip containing the QDs-in-polymer sample was mounted on a brass sample holder inside a low vibration, closed cycle optical cryostat (Montana Instruments Cryostation C2). An 0.85 NA objective was mounted on the cold-shield inside the cryostat at a temperature of 2040 K, allowing for a stable focal position and negligible radiation heating. The position of the sample was adjusted by a piezo-electric positioner (Attocube) inside the cryostat with 0.1 m resolution and 5 mm of travel in three dimensions. QDs were excited at either 473 nm with a continuous wave (CW) laser. QD emission is passed through a half-waveplate ($\lambda/2$) which is rotated by an angle θ to adjust the direction of polarization relative to the two detected orthogonal linear polarization components. An intermediate pinhole is used to select the region of emission, which is imaged into the input

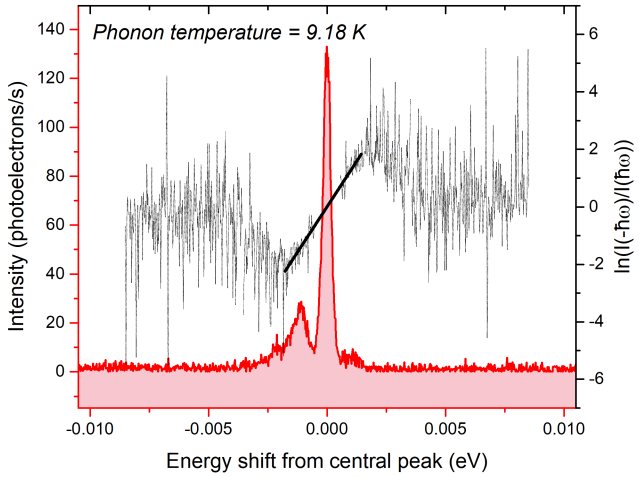

Figure S1: Trion spectrum obtained at 5K is plotted with respect to the shift from the central emission energy (shown in red). The intensity ratio $\ln\left(I(-\hbar\omega)/I(\hbar\omega)\right)$ is also plotted (shown in black) and the solid line is the linear fit over the range of phonon processes from which a phonon temperature of ≈ 9 K is obtained.

slit of an imaging spectrometer with 1.9 m focal length and a 1200 l/mm holographic grating. A polarization displacer splits the emission along the input slit into components polarized along and across the input slit, which is subsequently detected by a CCD camera with a spectral window of 34 meV at a resolution of 25 μeV per pixel. All measurements are done at 5 K unless mentioned otherwise.

S3 Phonon Temperature

Lineshape of the PL spectrum of the QD at cryogenic temperature is often a sharp ZPL superimposed by the broadband acoustic phonons.[2] The intensity of the broadband reflects the thermal distribution of phonons, described by the phonon population factor:

$$N_q = 1/(\exp(\frac{\hbar\omega}{k_B T}) - 1) \tag{S1}$$

At cryogenic temperatures, in the limit where multi-phonon processes are negligible, the phonon emission process proportional to (N_q+1) is dominant over phonon absorption process proportional to N_q, resulting in the asymmetric broadband visible in trion spectrum (See

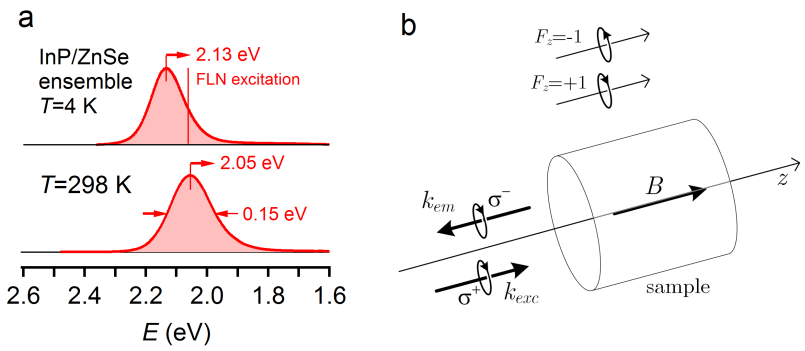

Figure S2: (a) Emission spectrum of the InP/ZnSe QD ensemble used for the FLN measurements as recorded at (bottom) 298 K and (top) 4 K. (b) Schematic outline of Faraday configuration used during the fluorescence line narrowing measurements, where the direction of the magnetic field is used to determine the z axis and, accordingly, the $F_z = +1$ and $F_z = -1$ states as indicated. According to these conventions, σ^+ circularly polarized light will excite the $F_z = +1$ state, whereas recombination from the $F_z = -1$ will yield emitted light with a σ^- circular polarization.

Figure S1) where the phonon emission is observed at lower energy to ZPL and phonon absorption at higher energy to ZPL. In PL experiments with the ZPL taken as the zero of frequency[3],

$$\ln\left(\frac{I(-\hbar\omega)}{I(\hbar\omega)}\right) = \frac{\omega}{k_B T} \tag{S2}$$

This intensity ratio is also included in Figure S1 which is fitted with a linear function (with intercept fixed to zero), from which we determine a phonon temperature of ≈ 9 K.

S4 Fluorescence Line Narrowing Spectroscopy

Sample Characteristics. For the fluorescence line narrowing (FLN), we used an ensemble of InP/ZnSe QDs synthesized using the approach as outlined in section S1. As shown in Figure S2a, the emission of ensemble was centered around 2.05 eV at room temperature and at 2.13 eV at 4 K. The excitation wavelength used for FLN spectroscopy thus overlapped with the low energy tail of the ensemble emission spectrum.

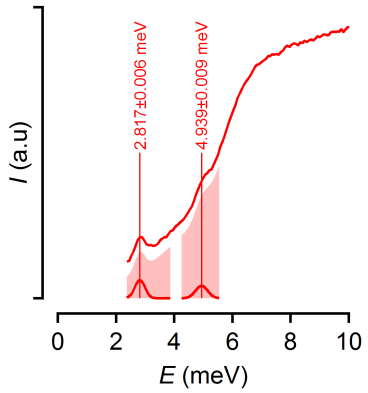

Figure S3: Fluorescence line narrowing (FLN) spectrum of an ensemble of InP/ZnSe QDs excited using 2.06 eV, σ^+ polarized light in a magnetic field of 22 T. The filled area show the best (local) fit of the spectrum to Eq S3, including a separate plot of the best fitting Gaussian and the resulting central emission energy E_0. The best fits have been offset for clarity.

Measurement setup. FLN experiments at low temperatures were performed at the High Field Magnet Laboratory (Radboud University, Nijmegen, The Netherlands). For these experiments, QD films dropcast on crystalline silicon substrate were used, which were mounted in a titanium sample holder on top of a three-axis piezo-positioner. The FLN measurements were performed in a Faraday configuration (see Figure S2b) using a spectrally narrow excitation source, achieved by using a tunable jet-stream dye (Rhodamine 6G) laser. This monochromatic laser beam was circularly polarized by means of a linear polarizer and a Babinet-Soleil compensator. The laser beam was focused on the sample by a singlet lens (10 mm focal length). The same lens was used to collect the PL emission and direct it to the detection setup (backscattering geometry). The samples and optical probe were mounted inside a liquid-helium bath cryostat. The high-resolution FLN emission was detected in crossed polarization mode relative to the laser polarization by using a linear polarizer and a lambda-quarter wave plate. The resonant-PL emission was analyzed by a 0.5 m long triple-grating spectrometer (3×1800 grooves/mm holographic gratings) in subtractive mode, equipped with a liquid nitrogen cooled CCD camera (Symphony-Horiba).

Spectrum Analysis. We estimated the central wavelength of the shifting emission features in the FLN spectrum by locally fitting the intensity $I(E)$ to a sum of a Gaussian and a quadratic background:

$$I(E) = A \exp\left(\frac{E - E_0}{w}\right)^2 + a_0 + a_1(E - E_0) + a_2(E - E_0)^2 \tag{S3}$$

Figure S3 shows an example of local fits of the FLN spectrum recorded at a field strength of 22 T. The resulting central wavelength of the respective emission features have been used to construct Figure 6 in the main text.

S5 The Isotropic Exciton in a Magnetic Field

When we take the 8 direct product states of the conduction-band electron and the valence-band hole as a basis (see Figure 1c), the exchange interaction couples states with the same angular momentum component F_z into different isotropic exciton states.[4] Taking the example of the $F_z = +1$ states, the two basis states can be defined as:

$$|\,0\,\rangle = |\,\frac{1}{2}\,\rangle_e |\,\frac{1}{2}\,\rangle_h \tag{S4}$$

$$|\,1\,\rangle = |\,-\frac{1}{2}\,\rangle_e |\,\frac{3}{2}\,\rangle_h \tag{S5}$$

Using this convention, the Hamiltonian operator $\mathbf{H}$ reads:[4]

$$\mathbf{H} = \begin{pmatrix} -\frac{1}{2}\eta & -i\sqrt{3}\eta \\ i\sqrt{3}\eta & \frac{3}{2}\eta \end{pmatrix} \tag{S6}$$

Here, η is a measure of the strength of the exchange interaction. The eigenenergies of $\mathbf{H}$ correspond to a bright high energy state $E_U = 5/2\eta$ and a dark low energy state $E_L = -3\eta/2$, as can be seen in Figure 1d for $\Delta = 0$. In the case of an isotropic exciton, the direction of the magnetic field can be taken as the z-axis, which means that the Zeeman Hamiltonian is

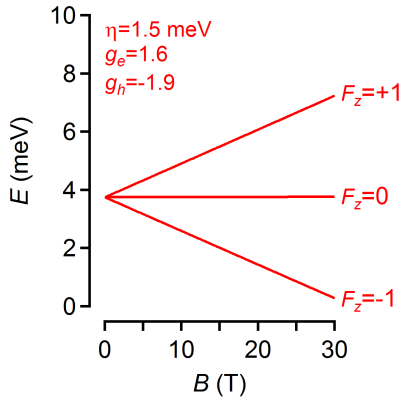

Figure S4: Representation of the energy of the bright isotropic exciton states $F_z = +1$, $F_z = +1$ and $F_z = +1$ state as a function of the applied magnetic fields, calculated using the parameters η, g_e and g_h as indicated.

diagonal in the give basis.[4] For the $F_z = +1$ states, we thus have:

$$\mathbf{H} = \begin{pmatrix} -\frac{1}{2}\eta + \mu_B B_z \frac{g_e - g_h}{2} & -i\sqrt{3}\eta \\ i\sqrt{3}\eta & \frac{3}{2}\eta - \mu_B B_z \frac{g_e + 3g_h}{2} \end{pmatrix} \tag{S7}$$

The upper eigenenergies $E_{1,U}$ of this Hamiltonian reads:

$$E_{1,U} = \frac{1}{2}\eta - g_h \mu_B B_z + \sqrt{3\eta^2 + \left(\eta^2 - \frac{g_e + g_h}{2}\mu_B B_z\right)^2} \tag{S8}$$

Figure S4 represents the energy of the $E_{1,U}$ state for a given set of parameters η, g_e and g_h.

For the $F_z = 0$ states, we can similarly define the basis states as:

$$|\,0\,\rangle = |\,\frac{1}{2}\,\rangle_e |\,-\frac{1}{2}\,\rangle_h \tag{S9}$$

$$|\,1\,\rangle = |\,-\frac{1}{2}\,\rangle_e |\,\frac{3}{2}\,\rangle_h \tag{S10}$$

In that case, the Hamiltonian operator in the presence of a magnetic field reads:[4]

$$\mathbf{H} = \begin{pmatrix} \frac{1}{2}\eta + \mu_B B_z \frac{g_e + g_h}{2} & -i2\eta \\ i2\eta & \frac{1}{2}\eta - \mu_B B_z \frac{g_e + g_h}{2} \end{pmatrix} \tag{S11}$$

In this case, we obtain the upper eigenenergy as (see Figure S4):

$$E_{0,U} = \frac{1}{2}\eta + \sqrt{4\eta^2 + \left(\frac{g_e + g_h}{2}\mu_B B_z\right)^2} \tag{S12}$$

Finally, for the $F_z = -1$ states, we start from the basis states defined as:

$$|\,0\,\rangle = |\,\frac{1}{2}\,\rangle_e|\,-\frac{3}{2}\,\rangle_h \tag{S13}$$

$$|\,1\,\rangle = |\,-\frac{1}{2}\,\rangle_e|\,-\frac{1}{2}\,\rangle_h \tag{S14}$$

In that case, the Hamiltonian operator in the presence of a magnetic field reads:[4]

$$\mathbf{H} = \begin{pmatrix} \frac{3}{2}\eta + \mu_B B_z \frac{g_e+3g_h}{2} & -i\sqrt{3}\eta \\ i\sqrt{3}\eta & -\frac{1}{2}\eta - \mu_B B_z \frac{g_e-g_h}{2} \end{pmatrix} \tag{S15}$$

In this case, we obtain the upper eigenenergy as (see Figure S4):

$$E_{-1,U} = \frac{1}{2}\eta + g_h\mu_B B_z + \sqrt{3\eta^2 + \left(\eta^2 + \frac{g_e + g_h}{2}\mu_B B_z\right)^2} \tag{S16}$$

S6 Fitting the Experimental Data to the Isotropic Exciton Model

Using the expressions derived in section S5 for $E_{1,U}$, $E_{0,U}$ and $E_{-1,U}$ (Eqs S8, S12, and S16, respectively), we can write the magnetic field induced splitting between these exciton states as (see Eqs 3 and 4):

$$\Delta E_{1,0} = -g_h\mu_B B + \sqrt{3\eta^2 + (\eta - \frac{g_e + g_h}{2}\mu_B B)^2} - \sqrt{4\eta^2 + (\frac{g_e + g_h}{2}\mu_B B)^2} \tag{S17}$$

$$\Delta E_{1,-1} = -2g_h\mu_B B + \sqrt{3\eta^2 + (\eta - \frac{g_e + g_h}{2}\mu_B B)^2} - \sqrt{3\eta^2 + (\eta + \frac{g_e + g_h}{2}\mu_B B)^2} \tag{S18}$$

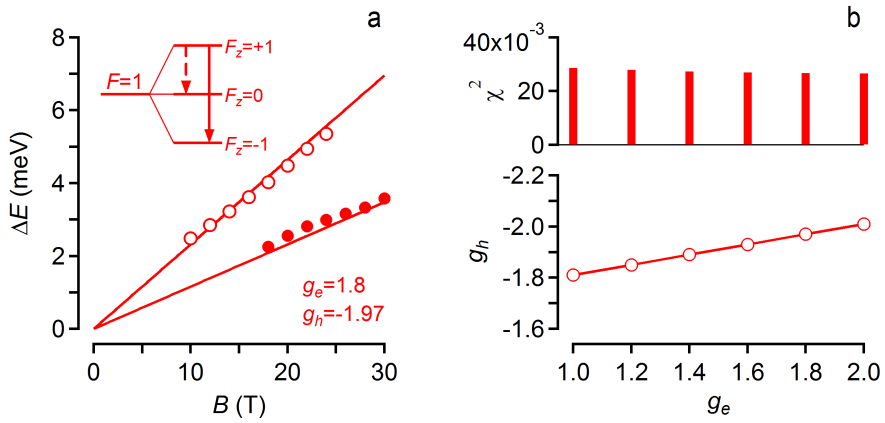

Figure S5: (a) Example of a global fit of the experimental data, where g_e was fixed at 1.8. (b) (bottom) Best fit values for g_h as obtained by a global fit of the experimental data as a function of the set value for g_e and (top) Mean square residuals for the best global fit as a function of the set value for g_e.

While these expressions depend in principle on 3 variables, *i.e.*, η, g_e and g_h, a global fit of the experimental data to Eqs S17 and S18 does not yield well-defined values for these variables, a problem that persists when η is fixed at 1.5 meV so as to yield the experimental dark-bright splitting. In Figure S5a, we represent an example of a global fit, where g_e was in addition set at 1.8 and g_h was used as the only adjustable parameter. Clearly, the result is not very different from the global fit shown in Figure 6c. This point is confirmed by Figure S5b, which shows that the mean square deviation between the experimental and fitted data hardly changes when g_e is varied from 1.0 to 2.0. On the other hand, this variation of g_e has little effect on the best fit value of g_h, which decreases from -1.8 to -2.0 across this g_e range. Hence, the conclusion that -1.9 ± 0.1 can be taken as a reasonable estimate for g_h.

S7 An Estimate of the Hole g-Factor

In defining the hole g-factor, we use the sign convention that when $g_h > 0$, the lowest hole state is the state with positive F_z.[5] According to Efros, the g-factor of a hole localized in a

spherically symmetric potential can be calculated as:[4]

$$g_h = \frac{4}{5}\gamma_1 I_2 + \frac{8}{5}\gamma(I_1 - I_2) + 2(\frac{5}{3}\gamma - \frac{1}{3}\gamma_1 - \frac{2}{3})(1 - \frac{4}{5}I_2) \tag{S19}$$

Here, I_1 and I_2 are integrals that can be calculated from the hole envelope wavefunction, whereas γ_1 and γ are Luttinger parameters. In the case that $\beta = 0.149$, the integrals I_1 and I_2 are approximately equal to -0.95 and 0.3, respectively.[4] With the Luttinger parameters $\gamma_1 = 5.1$ and $\gamma = 1.65$ for InP,[6] we thus calculate:

$$g_h \approx -1.49 \tag{S20}$$

References

1. Tessier, M. D.; Dupont, D.; De Nolf, K.; De Roo, J.; Hens, Z. Economic and Size-Tunable Synthesis of InP/ZnE (E = S, Se) Colloidal Quantum Dots. *Chem. Mater.* **2015**, *27*, 4893–4898.

2. Besombes, L.; Kheng, K.; Marsal, L.; Mariette, H. Acoustic phonon broadening mechanism in single quantum dot emission. *Phys. Rev. B* **2001**, *63*, 155307.

3. Zimmermann, R.; Muljarov, E. Dephasing of optical transitions in quantum dots Where exact solutions meet sophisticated experiments. Nanostructures: Physics and Technology. 2004; p 3.

4. Efros, A. L.; Rosen, M.; Kuno, M.; Nirmal, M.; Norris, D. J.; Bawendi, M. Band-Edge Exciton in Quantum Dots of Semiconductors with a Degenerate Valence Band: Dark and Bright Exciton States. *Phys. Rev. B* **1996**, *54*, 4843–4856.

5. Shornikova, E. V.; Biadala, L.; Yakovlev, D. R.; Feng, D.; Sapega, V. F.; Flipo, N.; Golovatenko, A. A.; Semina, M. A.; Rodina, A. V.; Mitioglu, A. A. *et al.* Electron and

Hole g-Factors and Spin Dynamics of Negatively Charged Excitons in CdSe/CdS Colloidal Nanoplatelets with Thick Shells. *Nano Letters* **2018**, *18*, 373–380.

6. Hackenberg, W.; Phillips, R. T.; Hughes, H. P. Investigation of the Luttinger Parameters for InP Using Hot-Electron Luminescence. *Phys. Rev. B* **1994**, *50*, 10598–10607.